EUROPEAN ORGANIZATION FOR NUCLEAR RESEARCH

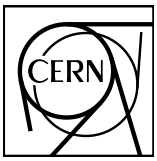

CERN-EP-2022-210
11 October 2022

$\psi(2S)$ suppression in Pb–Pb collisions at the LHC

ALICE Collaboration

Abstract

The production of the $\psi(2S)$ charmonium state was measured with ALICE in Pb–Pb collisions at $\sqrt{s_{\rm NN}} = 5.02$ TeV, in the dimuon decay channel. A significant signal was observed for the first time at LHC energies down to zero transverse momentum, at forward rapidity ($2.5 < y < 4$). The measurement of the ratio of the inclusive production cross sections of the $\psi(2S)$ and J/ψ resonances is reported as a function of the centrality of the collisions and of transverse momentum, in the region $p_{\rm T} < 12$ GeV/c. The results are compared with the corresponding measurements in pp collisions, by forming the double ratio $[\sigma^{\psi(2S)}/\sigma^{J/\psi}]_{\rm Pb-Pb}/[\sigma^{\psi(2S)}/\sigma^{J/\psi}]_{\rm pp}$. The $\psi(2S)$ nuclear modification factor $R_{\rm AA}$ was also obtained as a function of both centrality and $p_{\rm T}$. The results show that the $\psi(2S)$ resonance yield is strongly suppressed in Pb–Pb collisions, by a factor up to ~ 3 with respect to pp. Furthermore, the $\psi(2S)$ suppression in Pb–Pb collisions is stronger than the one observed for the J/ψ by a factor ~ 2. Comparisons of cross section ratios with previous SPS findings by the NA50 experiment, and of $R_{\rm AA}$ with higher-$p_{\rm T}$ results at LHC energy are also reported. These results and the corresponding comparisons with calculations of transport and statistical models address questions on the existence and properties of charmonium states in the quark–gluon plasma formed in nuclear collisions at the LHC.

Quarkonia, the bound states of a heavy quark–antiquark pair, represent an important test bench for Quantum Chromodynamics (QCD), the theory of strong interactions [1]. The production process of the pair is governed by the hard scale corresponding to the quark mass and occurs on a very short time (~ 0.1 fm/c), while its binding is a soft process, characterized by timescales that can be an order of magnitude larger [2, 3]. Static properties of quarkonia, and in particular their complex spectroscopy, can be reproduced by formulating QCD on a discrete lattice in space and time [4]. The quarkonium states can also be used as a probe of strongly interacting extended systems, and in particular of the quark–gluon plasma (QGP), a state of matter where quarks and gluons are deconfined over distances much larger than the hadronic size (~ 1 fm). In such a state, which can be created by collisions of heavy ions at ultrarelativistic energies, the large density of free color charges leads to a screening of the quark–antiquark binding and to the dissociation of quarkonia [5]. Effects related to a collisional damping of the states can also be present, leading to a loss of correlation in the pair and consequently to a modification of the spectral functions in the QGP [6]. Finally, the QGP created in the collision expands and cools down until it crosses the pseudocritical temperature T_c (of about 157 MeV for a system with zero net baryonic number [7, 8]) for the transition to a hadronic phase. Close to this transition, if the initial multiplicity of heavy quark pairs is large, recombination processes, which counterbalance to a certain extent the suppression in the QGP, may become sizeable [9, 10], i.e. quarks and antiquarks close in phase space can recombine to form a quarkonium state. These processes may already be effective even in the QGP phase [11].

A further important element in the study of quarkonium production in heavy-ion collisions is their rich variety of states. Restricting the discussion to charmonia, bound states of charm–anticharm quarks, the ground level J/ψ vector meson and its radial excitation ψ(2S) differ in binding energy by more than a factor 10 (~ 640 vs ~ 50 MeV, respectively) and by about a factor 2 in size [12, 13]. As a consequence, a sequential suppression of the charmonium states in the QGP [14] with increasing temperature of the medium and according to their binding energy was predicted. Also the recombination processes might in principle have different features, with the larger-size charmonium states being produced later in the evolution of the system [15]. Current theoretical approaches for the complex phenomenology of charmonium production in nuclear collisions include transport models [16, 17], where dissociation/recombination rates for quarkonium states in the QGP are calculated taking into account a lattice-QCD inspired evaluation of the dependence of their spectral properties on the evolving thermodynamic properties of the medium. In the Statistical Hadronization Model (SHMc) [18], charmonia are assumed to be formed at hadronization according to statistical weights and introducing a charm fugacity factor related to charm conservation and determined by its production cross section[1]. The availability of accurate experimental results for various charmonium states represents a crucial input for the evaluation of the theory approaches and ultimately for the understanding of the existence of bound states of heavy quarks in the QGP.

On the experimental side, a suppression of the J/ψ in Pb–Pb collisions was observed by the NA50 experiment at the CERN SPS [19] (center of mass energy per nucleon–nucleon collision $\sqrt{s_{\rm NN}} = 17.3$ GeV) and subsequently confirmed at RHIC by PHENIX [20] and STAR [21] (Au–Au at $\sqrt{s_{\rm NN}} = 200$ GeV). At the LHC (Pb–Pb at $\sqrt{s_{\rm NN}} = 2.76$ and 5.02 TeV), the ALICE Collaboration has unambiguously demonstrated the existence and role of the recombination processes, by observing at low transverse momentum ($p_{\rm T}$), and in central collisions, a smaller suppression compared to lower-energy results [22]. At high $p_{\rm T}$, CMS and ATLAS results indicate a strong J/ψ suppression [23, 24], reaching a value of ~ 4 for central collisions, where the geometric overlap of the colliding nuclei is maximal. The suppression in Pb–Pb collisions is quantified via the nuclear modification factor $R_{\rm AA}$, defined as the ratio between the J/ψ yield in Pb–Pb and the product of the corresponding J/ψ cross section in pp collisions times the average nuclear thickness function $\langle T_{\rm AA} \rangle$ [25], a quantity proportional to the number of nucleon–nucleon collisions.

[1] In the frame of SHMc it can be more appropriate to use the word "combination" rather than "recombination" as there is no binding of charmonium states in the QGP phase.

The $\psi(2S)$ measurements are more challenging, due to the ~ 7.5 lower branching ratio to muon pairs with respect to the J/ψ, and the ~ 6 times smaller production cross section in pp collisions at LHC energy [26]. The most accurate result until today was obtained by NA50, which measured a decrease of the cross section ratio between $\psi(2S)$ and J/ψ by a factor ~ 2, when increasing the collision centrality. Both transport [11, 27] and statistical hadronization models [28] were able to reproduce the main features of this result (see e.g. Fig. 37 of Ref. [29]). More recently, $\psi(2S)$ production was studied by ATLAS [23] and CMS [24, 30], measuring the double ratio between the $\psi(2S)$ and J/ψ cross sections in Pb–Pb and pp collisions at $\sqrt{s_{\rm NN}} = 5.02$ TeV. Their analyses, carried out at midrapidity, show in the high-$p_{\rm T}$ region a strong relative suppression of the $\psi(2S)$ with respect to J/ψ, by a factor ~ 2. For a complete characterization of $\psi(2S)$ production at these energies, an extension of these results towards low $p_{\rm T}$, the kinematic region where recombination effects are maximal, is needed. To date, the previous result by ALICE [31] at $\sqrt{s_{\rm NN}} = 2.76$ TeV does not allow a firm conclusion, due to the large uncertainties.

In this Letter, we present a measurement of inclusive $\psi(2S)$ production, carried out by ALICE in Pb–Pb collisions at $\sqrt{s_{\rm NN}} = 5.02$ TeV. The $\psi(2S)$ is studied by means of its decay to muon pairs in the region $2.5 < y < 4$ and down to $p_{\rm T} = 0$. Results are given on the (double) ratio of production cross sections between the $\psi(2S)$ and J/ψ, as well as on the $\psi(2S)$ $R_{\rm AA}$. The ALICE detector is described extensively in Refs. [32, 33]. In particular, muon detection is carried out by a forward spectrometer consisting of a 3 Tm dipole magnet, a system of two hadron absorbers, five tracking (Cathode Pad Chambers) and two triggering (Resistive Plate Chambers) stations. The minimum-bias (MB) trigger is obtained as a coincidence of signals from the two V0 scintillator arrays ($-3.7 < \eta < -1.7$ and $2.8 < \eta < 5.1$), also used for the rejection of beam–gas interactions and for the determination of the centrality of the collisions (see below).

The data analyzed in this Letter were collected in 2015 and 2018, and correspond to an integrated luminosity $L_{\rm int} \sim 750\ \mu{\rm b}^{-1}$. The collisions were classified from central to peripheral according to the decreasing energy deposition in the V0 detectors, which can be related to the degree of geometric overlap of the colliding nuclei [25, 34]. Events were recorded using a dimuon trigger, given by the coincidence of a MB trigger together with the detection of two opposite-sign tracks in the triggering system of the muon spectrometer. The trigger algorithm applies a non-sharp $p_{\rm T}$ threshold, which has 50% efficiency at 1 GeV/c and becomes fully efficient ($> 98\%$) for $p_{\rm T} > 2$ GeV/c. Selection criteria were applied at the single muon and muon pair levels (see Ref. [35] for details). In particular, tracks reconstructed in the tracking system were required to point to the interaction vertex and to match a corresponding track in the trigger system. The radial position of the tracks at the end of the front absorber must be in the range $17.6 < R < 89.5$ cm and their pseudorapidity range within $-4 < \eta_\mu < -2.5$. Opposite-sign dimuons were selected in the rapidity interval $2.5 < y < 4$ [2].

The number of reconstructed $\psi(2S)$, as well as that of J/ψ, was obtained by means of χ^2 minimization fits of the opposite-sign dimuon invariant-mass spectra. The combinatorial background was subtracted with the help of an event mixing procedure, described in detail in Ref. [31]. The resonance signals were described by a double-sided Crystal Ball function or a pseudo-Gaussian with a mass-dependent width [36]. The position of the pole mass of the J/ψ, as well as its width, were kept as free parameters in the fitting procedure. For the $\psi(2S)$, due to the much smaller statistical significance of its signal, its mass was bound to that of the J/ψ, via the mass difference of the two resonances as provided by the Particle Data Group [37], $m_{\psi(2S)} = m^{\rm FIT}_{{\rm J}/\psi} + (m^{\rm PDG}_{\psi(2S)} - m^{\rm PDG}_{{\rm J}/\psi})$. The width was also bound to that of the J/ψ, imposing the same ratio of the J/ψ and $\psi(2S)$ widths as the one measured in the data sample of pp collisions at $\sqrt{s} = 13$ TeV [38] or in Monte Carlo (MC) simulations (see details below). The same data sample, or the MC, were also used to fix the non-Gaussian tails of the resonance mass spectra. The continuum component of the correlated background remaining in the dimuon distributions after mixed-event subtraction and originating mainly from semi-muonic decays of pairs of heavy-flavor hadrons, was

[2] Due to the symmetry of the collision system, a positive sign notation was adopted.

parametrized using various empirical functions. Fits were performed in two invariant mass intervals, centered in the resonance region. The resonance signals were extracted in four $p_{\rm T}$ classes for the centrality range 0–90% and in four centrality classes. For the latter series, the selections $p_{\rm T} < 12$ GeV/c and $0.3 < p_{\rm T} < 12$ GeV/c were used for the two most central and peripheral classes, respectively, to remove the low-$p_{\rm T}$ contribution from photoproduction [39] which becomes important for peripheral collisions. The minimum significance of the ψ(2S) signal as a function of centrality is 7.6 (60–90%) and increases by a factor ~ 8 for central events. The corresponding numbers for the $p_{\rm T}$ dependence are 11.3 at high $p_{\rm T}$ increasing by a factor ~ 3 at low $p_{\rm T}$. For each kinematic and/or centrality selection, the numbers of detected ψ(2S) and J/ψ were obtained by averaging the results of the various fits. For the complete data sample (0–90%) they amount to 1.3×10^4 and 9.2×10^5, respectively.

The product of acceptance times efficiency ($A \times \varepsilon$) has been calculated by means of a MC simulation. The $p_{\rm T}$ and y distributions for the generated J/ψ were matched to those extracted from data using an iterative procedure as done in Ref. [40], and the same distributions were also used for the ψ(2S). The misalignment of the detection elements as well as the time-dependent status of each electronic channel during the data taking period were taken into account in the simulation. The resonance signals were embedded into real events in order to properly reproduce the effect of detector occupancy and its variation from one centrality class to another, and then reconstructed. The centrality and $p_{\rm T}$-integrated $A \times \varepsilon$ values are 13.5% and 17.3% for J/ψ and ψ(2S). As a function of $p_{\rm T}$ and centrality the $A \times \varepsilon$ vary within a factor ~ 2 and by about 5%, respectively.

The evaluation of the double ratios and the nuclear modification factors requires the measurement of the charmonium cross sections in pp collisions at $\sqrt{s} = 5.02$ TeV. Results from Ref. [41] were used for this purpose, by appropriately combining, where necessary, the ψ(2S) cross sections and the ratios $\sigma_{\psi(2S)}/\sigma_{J/\psi}$, in order to match the $p_{\rm T}$ binning used in this analysis.

The normalization of the yields per event in Pb–Pb collisions is obtained calculating the number of "equivalent" minimum-bias events as the product of the number of dimuon-triggered events ($\sim 4 \times 10^8$) times the inverse of the probability of having a dimuon trigger in a MB event (F), following the procedure described e.g., in Ref. [42]. For the 0–90% centrality class, the value of the normalization factor is $F = 13.1 \pm 0.1$. Finally, the $< T_{\rm AA} >$ values were taken from Ref. [25] for the centrality intervals directly quoted there, or by combining their values for the other intervals.

Table 1: Contributions to the systematic uncertainties (in percentage). Values with an asterisk correspond to the systematic uncertainties correlated as a function of the given variable. The pp reference entry includes a 1.8% luminosity uncertainty.

	vs centrality	vs $p_{\rm T}$
	ψ(2S) $R_{\rm AA}$	
Signal extraction	16–22	12–25
Tracking effic.	3 *	3
Trigger effic.	1.6 *	1.5–2
Matching effic.	1 *	1
MC input	2 *	2
F	0.7 *	0.7 *
$\langle T_{\rm AA} \rangle$	0.7–2.3	1 *
Centrality	0–7	0.3 *
pp ref.	4.7 *	7.9–11.1
	(Double) ratios	
Signal extraction	16–23	12–24
pp ref.	6.7 *	5.5–8.8

A summary of the systematic uncertainties affecting the calculation of the (double) ratios and $\psi(2S)$ R_{AA} is given in Table 1. They were obtained following similar procedures as those adopted for previous charmonium analyses at forward rapidity, that are detailed e.g., in Refs. [43, 44]. For the signal extraction, the systematic uncertainty was calculated as the root mean square of the values of the number of $\psi(2S)$ obtained by combining different fitting ranges, signal and residual background shapes. In addition, two different normalization ranges of the mixed-event spectra were tested. Fits with a $\chi^2/\mathrm{ndf} > 2.5$ were excluded from the calculation. Due to the very low signal over background values before mixed-event subtraction, down to less than 0.1%, a fit to the invariant mass distribution without subtraction of mixed-event background does not allow a robust signal extraction and has therefore not been used in this analysis. For the ingredients entering the $A \times \varepsilon$ calculation, the systematic uncertainties related to tracking, triggering, and matching of candidate tracks between tracking and triggering detectors were obtained by comparing information obtained in MC and in data, as described in Ref. [44]. The uncertainty due to the generated y and p_T resonance shapes in the MC was estimated as in Ref. [40], taking into account the statistical uncertainty on the measured distributions used for their definition in the iterative procedure, and the possible correlations between the distributions in y and p_T. The uncertainty on F was obtained by comparing the results of two different evaluations as discussed in Ref. [42], while for $\langle T_{AA} \rangle$ they were computed by varying the input parameters of the Glauber calculation used for their estimate [25]. For the centrality evaluation, the systematic uncertainty was obtained varying by $\pm 1\%$ the value of the V0 signal amplitude corresponding to the most central 90% of the hadronic Pb–Pb cross section and re-extracting the resonance signal under this hypothesis, as detailed in Ref. [43]. For the pp reference, uncertainties were obtained by combining the corresponding values from the narrower p_T intervals reported in Ref. [41]. A further uncertainty related to the evaluation of the pp luminosity is also considered in the R_{AA} evaluation [41]. All the uncertainties discussed in this paragraph are added in quadrature to obtain the total systematic uncertainty.

When the $\psi(2S)$ to J/ψ cross section ratios are computed, all uncertainties cancel out except the one related to the signal extraction which is dominated by the former resonance. For the double ratios, the uncertainties on the pp cross section ratio between $\psi(2S)$ and J/ψ were also obtained starting from Ref. [41].

In Fig. 1 the ratio of $\psi(2S)$ and J/ψ cross sections (not corrected for the branching ratios of the dimuon decay) is shown as a function of centrality, expressed as the average number of participant nucleons $\langle N_{part} \rangle$. In the lower panel, the values of the double ratio can be read, showing a $\psi(2S)$ suppression by a factor of about 50% with respect to pp. No significant centrality dependence of the results is seen, within the uncertainties. Comparison with calculations of a transport approach (TAMU) [15] and of the SHMc model [18, 45] are also shown. The TAMU model reproduces the cross section ratios over centrality, while the SHMc model tends to underestimate the data in central Pb–Pb collisions. The ALICE results are also compared with the corresponding (double) ratios obtained by NA50 in $0 < y < 1$ [46], which reach smaller values for central events.

In Fig. 2 the nuclear modification factors for $\psi(2S)$ (this analysis) and J/ψ (from Ref. [43]) are compared, as a function of $\langle N_{part} \rangle$. Due to the limited number of centrality intervals that could be defined, the R_{AA} values for the $\psi(2S)$ do not show a clear trend and are generally consistent with an R_{AA} value of about 0.4. In Fig. 2 calculations with the TAMU model are also shown, indicating a good agreement with the measured R_{AA} for both J/ψ and $\psi(2S)$. The SHMc model reproduces, within uncertainties, the J/ψ R_{AA} centrality dependence, while it underestimates the $\psi(2S)$ production in central and semi-central collisions.

In Fig. 3 the p_T-dependence of the ratio of the $\psi(2S)$ and J/ψ production cross sections for Pb–Pb collisions, in 0–90% centrality, is presented and compared to the corresponding pp results. Both the Pb–Pb and pp ratios increase as a function of p_T, with a milder rise in the former case. The double ratio values are also shown, indicating a significant relative suppression of the $\psi(2S)$, slightly increasing with

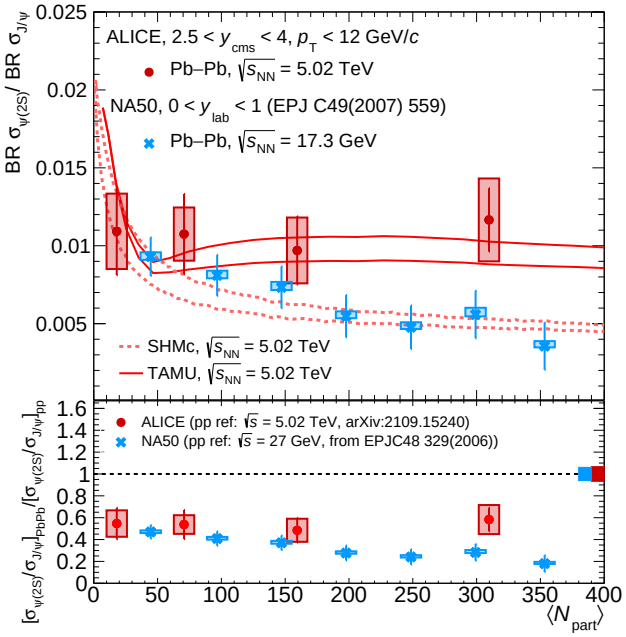

Figure 1: Ratio of the $\psi(2S)$ and J/ψ cross sections as a function of $\langle N_{\rm part}\rangle$. To remove the contamination from photoproduced charmonium, only $\psi(2S)$ and J/ψ having $p_{\rm T} > 0.3$ GeV/c are considered in the two most peripheral classes. The vertical error bars and the filled boxes represent statistical and systematic uncertainties, respectively. In the lower panel the ratios are normalized to the corresponding pp value (double ratio). Data are compared to predictions of the TAMU [15] and SHMc [18, 45] models and to results of the SPS NA50 experiment [46]. The filled boxes around the line at unity indicate the global systematic uncertainties.

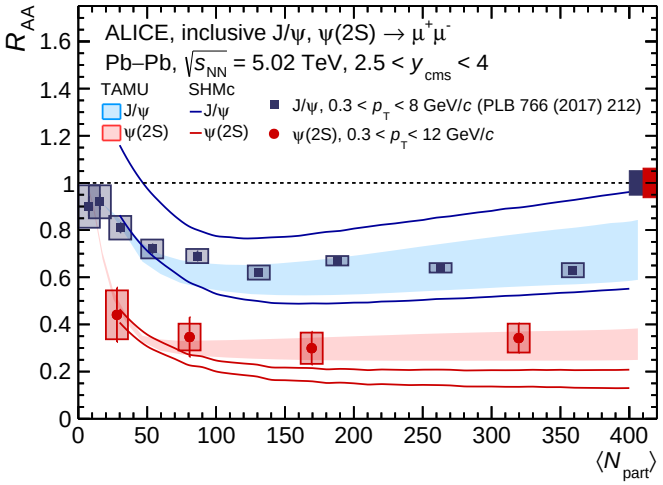

Figure 2: The $R_{\rm AA}$ for the $\psi(2S)$ (this analysis) and J/ψ [43] as a function of $\langle N_{\rm part}\rangle$. Comparisons with theory models are also shown.

$p_{\rm T}$ up to a value of ~ 0.5.

Figure 4 shows the $\psi(2S)$ $R_{\rm AA}$, compared with the corresponding result for the J/ψ [44], as a function of $p_{\rm T}$. The corresponding CMS measurements [47] in the region $|y| < 1.6$ and $6.5 < p_{\rm T} < 30$ GeV/c are also

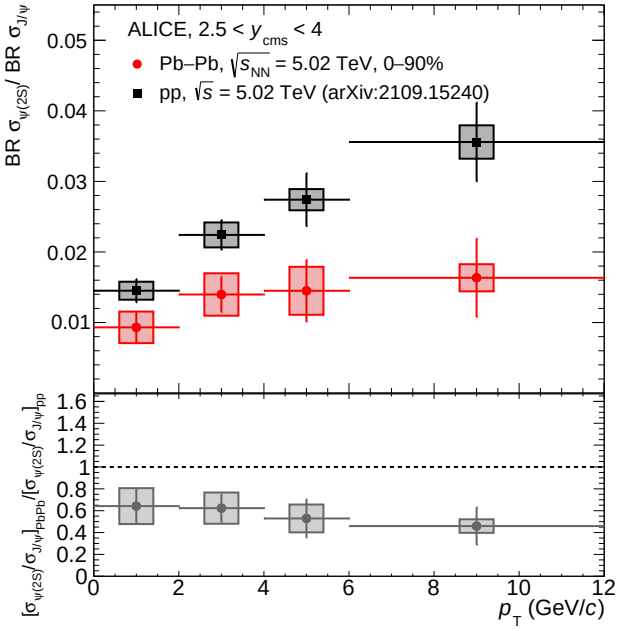

Figure 3: The ratio of the $\psi(2S)$ and J/ψ cross sections as a function of p_T, compared to measurements in pp collisions [41]. In the lower panel the double ratios of the Pb–Pb and pp values is shown.

reported. The main feature is an increase of the nuclear modification factor at low p_T, similar to what was observed for the J/ψ and understood as a direct consequence of the recombination process of charm and anticharm quarks. The strong suppression of the $\psi(2S)$ ($R_{AA} \sim 0.15$ at $p_T = 10$ GeV/c) persists up to $p_T = 30$ GeV/c as shown by the CMS data, that agree within uncertainties with those of ALICE in the common p_T range, in spite of the different rapidity coverage. A comparison with predictions from the TAMU model [15] is shown, indicating that also the p_T dependence of the R_{AA} is well reproduced for both J/ψ and $\psi(2S)$, as it was the case for the centrality dependence.

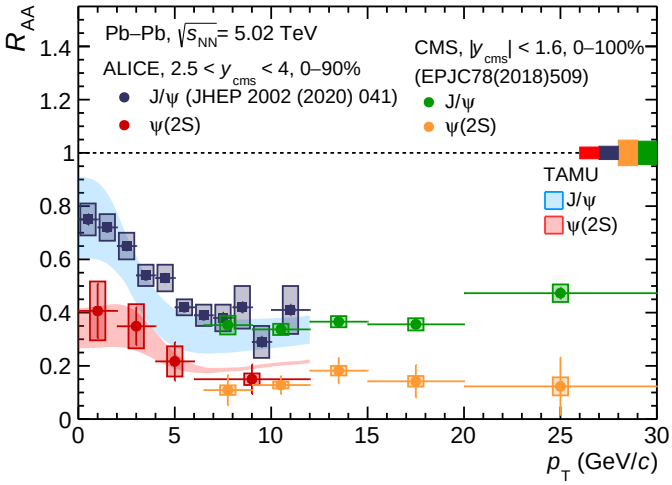

Figure 4: The R_{AA} for $\psi(2S)$ and J/ψ [43] as a function of p_T. Comparison with theory models and results from the CMS experiment [30] are also shown.

The picture emerging from these results shows a clear hierarchy of suppression of J/ψ and ψ(2S) over the whole $p_{\rm T}$ and centrality intervals explored. Apart from the overall larger ψ(2S) suppression, visible in the double ratios and in the comparison of the $R_{\rm AA}$, no significant difference in the $p_{\rm T}$ and centrality dependence of the suppression effects between the two states can be seen. The comparison with SPS results reveals that such a suppression in central events tends to be stronger at low collision energy compared to LHC. When comparing the results with the predictions of transport and statistical models a fair agreement is obtained, with the transport approach better reproducing the ALICE results for central events.

In summary, we have provided a first accurate measurement of ψ(2S) production in Pb–Pb collisions at LHC energy down to zero $p_{\rm T}$, in the rapidity region $2.5 < y < 4$. Results on the cross section ratios between ψ(2S) and J/ψ, on the double ratio between Pb–Pb and pp collisions, and on the nuclear modification factors were shown. A relative suppression by a factor ~ 2 of the ψ(2S) with respect to the J/ψ is observed, with no significant $p_{\rm T}$ or centrality dependence within the uncertainties. The $R_{\rm AA}$ values for the ψ(2S) show a hint for a decrease as a function of $p_{\rm T}$, reminiscent of the same effect observed for the J/ψ and connected with charm quark recombination processes. As a function of centrality, values around $R_{\rm AA} \sim 0.4$ are observed. The comparison with transport and statistical models shows a fair agreement. The transport model, that include recombination of charm quarks in the QGP phase, better reproduces the results for central events.

References

[1] N. Brambilla *et al.*, "Heavy quarkonium: progress, puzzles, and opportunities", *Eur. Phys. J. C* **71** (2011) 1534, arXiv:1010.5827 [hep-ph].

[2] D. Kharzeev and R. L. Thews, "Quarkonium formation time in a model independent approach", *Phys. Rev. C* **60** (1999) 041901, arXiv:nucl-th/9907021.

[3] J. Hufner, Y. P. Ivanov, B. Z. Kopeliovich, and A. V. Tarasov, "Photoproduction of charmonia and total charmonium proton cross-sections", *Phys. Rev. D* **62** (2000) 094022, arXiv:hep-ph/0007111.

[4] **HPQCD, UKQCD, MILC, Fermilab Lattice** Collaboration, C. T. H. Davies *et al.*, "High precision lattice QCD confronts experiment", *Phys. Rev. Lett.* **92** (2004) 022001, arXiv:hep-lat/0304004.

[5] T. Matsui and H. Satz, "J/ψ Suppression by Quark-Gluon Plasma Formation", *Phys. Lett.B* **178** (1986) 416–422.

[6] M. Laine, O. Philipsen, P. Romatschke, and M. Tassler, "Real-time static potential in hot QCD", *JHEP* **03** (2007) 054, arXiv:hep-ph/0611300.

[7] **HotQCD** Collaboration, A. Bazavov *et al.*, "Chiral crossover in QCD at zero and non-zero chemical potentials", *Phys. Lett. B* **795** (2019) 15–21, arXiv:1812.08235 [hep-lat].

[8] S. Borsanyi, Z. Fodor, J. N. Guenther, R. Kara, S. D. Katz, P. Parotto, A. Pasztor, C. Ratti, and K. K. Szabo, "QCD Crossover at Finite Chemical Potential from Lattice Simulations", *Phys. Rev. Lett.* **125** no. 5, (2020) 052001, arXiv:2002.02821 [hep-lat].

[9] P. Braun-Munzinger and J. Stachel, "(Non)thermal aspects of charmonium production and a new look at J/ψ suppression", *Phys. Lett. B* **490** (2000) 196–202, arXiv:nucl-th/0007059 [nucl-th].

[10] R. L. Thews, M. Schroedter, and J. Rafelski, "Enhanced J/ψ production in deconfined quark matter", *Phys. Rev. C* **63** (2001) 054905, arXiv:hep-ph/0007323 [hep-ph].

[11] L. Grandchamp, R. Rapp, and G. E. Brown, "In medium effects on charmonium production in heavy ion collisions", *Phys. Rev. Lett.* **92** (2004) 212301, arXiv:hep-ph/0306077.

[12] F. Karsch and H. Satz, "The spectral analysis of strongly interacting matter", *Z. Phys. C* **51** (1991) 209–224.

[13] H. Satz, "Colour deconfinement and quarkonium binding", *J. Phys. G* **32** (2006) R25, arXiv:hep-ph/0512217.

[14] S. Digal, P. Petreczky, and H. Satz, "Quarkonium feed down and sequential suppression", *Phys. Rev. D* **64** (2001) 094015, arXiv:hep-ph/0106017 [hep-ph].

[15] X. Du and R. Rapp, "Sequential Regeneration of Charmonia in Heavy-Ion Collisions", *Nucl. Phys. A* **943** (2015) 147–158, arXiv:1504.00670 [hep-ph].

[16] X. Zhao and R. Rapp, "Medium Modifications and Production of Charmonia at LHC", *Nucl. Phys. A* **859** (2011) 114–125, arXiv:1102.2194 [hep-ph].

[17] K. Zhou, N. Xu, Z. Xu, and P. Zhuang, "Medium effects on charmonium production at ultrarelativistic energies available at the CERN Large Hadron Collider", *Phys. Rev. C* **89** no. 5, (2014) 054911, arXiv:1401.5845 [nucl-th].

[18] A. Andronic, P. Braun-Munzinger, M. K. Köhler, K. Redlich, and J. Stachel, "Transverse momentum distributions of charmonium states with the statistical hadronization model", *Phys. Lett. B* **797** (2019) 134836, arXiv:1901.09200 [nucl-th].

[19] **NA50** Collaboration, B. Alessandro *et al.*, "A new measurement of J/ψ suppression in Pb–Pb collisions at 158 GeV per nucleon", *Eur. Phys. J. C* **39** (2005) 335–345, arXiv:hep-ex/0412036 [hep-ex].

[20] **PHENIX** Collaboration, A. Adare *et al.*, "J/ψ suppression at forward rapidity in Au+Au collisions at $\sqrt{s_{\rm NN}} = 200$ GeV", *Phys. Rev. C* **84** (2011) 054912, arXiv:1103.6269 [nucl-ex].

[21] **STAR** Collaboration, J. Adam *et al.*, "Measurement of inclusive J/ψ suppression in Au+Au collisions at $\sqrt{s_{\rm NN}}$ = 200 GeV through the dimuon channel at STAR", *Phys. Lett. B* **797** (2019) 134917, arXiv:1905.13669 [nucl-ex].

[22] **ALICE** Collaboration, S. Acharya *et al.*, "Centrality and transverse momentum dependence of inclusive J/ψ production at midrapidity in Pb–Pb collisions at $\sqrt{s_{\rm NN}}$=5.02 TeV", *Phys. Lett. B* **805** (2020) 135434, arXiv:1910.14404 [nucl-ex].

[23] **ATLAS** Collaboration, M. Aaboud *et al.*, "Prompt and non-prompt J/ψ and ψ(2S) suppression at high transverse momentum in 5.02 TeV Pb+Pb collisions with the ATLAS experiment", *Eur. Phys. J.* **C78** no. 9, (2018) 762, arXiv:1805.04077 [nucl-ex].

[24] **CMS** Collaboration, A. M. Sirunyan *et al.*, "Relative Modification of Prompt ψ(2S) and J/ψ Yields from pp to PbPb Collisions at $\sqrt{s_{NN}} = 5.02$ TeV", *Phys. Rev. Lett.* **118** no. 16, (2017) 162301, arXiv:1611.01438 [nucl-ex].

[25] **ALICE** Collaboration, "Centrality determination in heavy ion collisions", ALICE-PUBLIC-2018-011. http://cds.cern.ch/record/2636623.

[26] **ALICE** Collaboration, B. Abelev *et al.*, "Measurement of quarkonium production at forward rapidity in pp collisions at $\sqrt{s} = 7$ TeV", *Eur. Phys. J. C* **74** no. 8, (2014) 2974, arXiv:1403.3648 [nucl-ex].

[27] L. Grandchamp, R. Rapp, and G. E. Brown, "Medium modifications of charm and charmonium in high-energy heavy ion collisions", *J. Phys. G* **30** (2004) S1355–S1358, arXiv:hep-ph/0403204.

[28] A. Andronic, P. Braun-Munzinger, K. Redlich, and J. Stachel, "Statistical hadronization of heavy quarks in ultra-relativistic nucleus-nucleus collisions", *Nucl. Phys. A* **789** (2007) 334–356, arXiv:nucl-th/0611023.

[29] R. Rapp and H. van Hees, *Heavy Quarks in the Quark-Gluon Plasma*, pp. 111–206 (2010). 2010. arXiv:0903.1096 [hep-ph].

[30] **CMS** Collaboration, A. M. Sirunyan *et al.*, "Measurement of prompt and nonprompt charmonium suppression in PbPb collisions at 5.02 TeV", *Eur. Phys. J. C* **78** no. 6, (2018) 509, arXiv:1712.08959 [nucl-ex].

[31] **ALICE** Collaboration, J. Adam *et al.*, "Differential studies of inclusive J/ψ and ψ(2S) production at forward rapidity in Pb–Pb collisions at $\sqrt{s_{\rm NN}} = 2.76$ TeV", *JHEP* **05** (2016) 179, arXiv:1506.08804 [nucl-ex].

[32] **ALICE** Collaboration, K. Aamodt *et al.*, "The ALICE experiment at the CERN LHC", *JINST* **3** (2008) S08002.

[33] **ALICE** Collaboration, B. Abelev *et al.*, "Performance of the ALICE Experiment at the CERN LHC", *Int. J. Mod. Phys. A* **29** (2014) 1430044, arXiv:1402.4476 [nucl-ex].

[34] **ALICE** Collaboration, B. Abelev *et al.*, "Centrality determination of Pb–Pb collisions at $\sqrt{s_{\rm NN}}$ = 2.76 TeV with ALICE", *Phys. Rev. C* **88** no. 4, (2013) 044909, arXiv:1301.4361 [nucl-ex].

[35] **ALICE** Collaboration, S. Acharya *et al.*, "Study of J/ψ azimuthal anisotropy at forward rapidity in Pb–Pb collisions at $\sqrt{s_{\rm NN}} = 5.02$ TeV", *JHEP* **02** (2019) 012, arXiv:1811.12727 [nucl-ex].

[36] **ALICE** Collaboration, J. Adam *et al.*, "Quarkonium signal extraction in ALICE", ALICE-PUBLIC-2015-006. https://cds.cern.ch/record/2060096.

[37] **Particle Data Group** Collaboration, R. L. Workman and Others, "Review of Particle Physics", *PTEP* **2022** (2022) 083C01.

[38] **ALICE** Collaboration, S. Acharya *et al.*, "Energy dependence of forward-rapidity J/ψ and ψ(2S) production in pp collisions at the LHC", *Eur. Phys. J. C* **77** no. 6, (2017) 392, arXiv:1702.00557 [hep-ex].

[39] **ALICE** Collaboration, "Photoproduction of low-$p_{\rm T}$ J/ψ from peripheral to central Pb$-$Pb collisions at 5.02 TeV", arXiv:2204.10684 [nucl-ex].

[40] **ALICE** Collaboration, S. Acharya *et al.*, "Inclusive J/ψ production at forward and backward rapidity in p–Pb collisions at $\sqrt{s_{\rm NN}}$ = 8.16 TeV", *JHEP* **07** (2018) 160, arXiv:1805.04381 [nucl-ex].

[41] **ALICE** Collaboration, S. Acharya *et al.*, "Inclusive quarkonium production in pp collisions at $\sqrt{s} = 5.02$ TeV", arXiv:2109.15240 [nucl-ex].

[42] **ALICE** Collaboration, S. Acharya *et al.*, "Z-boson production in p–Pb collisions at $\sqrt{s_{\rm NN}} = 8.16$ TeV and Pb–Pb collisions at $\sqrt{s_{\rm NN}} = 5.02$ TeV", *JHEP* **09** (2020) 076, arXiv:2005.11126 [nucl-ex].

[43] **ALICE** Collaboration, J. Adam *et al.*, "J/ψ suppression at forward rapidity in Pb–Pb collisions at $\sqrt{s_{\rm NN}} = 5.02$ TeV", *Phys. Lett. B* **766** (2017) 212–224, arXiv:1606.08197 [nucl-ex].

[44] **ALICE** Collaboration, S. Acharya *et al.*, "Studies of J/ψ production at forward rapidity in Pb–Pb collisions at $\sqrt{s_{\rm NN}}$ = 5.02 TeV", *JHEP* **02** (2020) 041, arXiv:1909.03158 [nucl-ex].

[45] A. Andronic, P. Braun-Munzinger, K. Redlich, and J. Stachel, "Decoding the phase structure of QCD via particle production at high energy", *Nature* **561** no. 7723, (2018) 321–330, arXiv:1710.09425 [nucl-th].

[46] **NA50** Collaboration, B. Alessandro *et al.*, "ψ' production in Pb–Pb collisions at 158 GeV/nucleon", *Eur. Phys. J. C* **49** (2007) 559–567, arXiv:nucl-ex/0612013.

[47] **CMS** Collaboration, A. M. Sirunyan *et al.*, "Measurement of prompt and nonprompt charmonium suppression in PbPb collisions at 5.02 TeV", *Eur. Phys. J. C* **78** no. 6, (2018) 509, arXiv:1712.08959 [nucl-ex].